ESTA JOURNAL
Energy Storage Technology and Applications

Article

jurnal.uns.ac.id/esta

Comparative Study of Novel Thin-films for Li-ion Batteries

M. N. Ikhsanudin[1,3], S. S. Nisa[3], A. Jamaluddin[2,3,*]

1. Department of Chemical Engineering, Faculty of Engineering, Universitas Sebelas Maret, Surakarta 57126, Central Java, Indonesia
2. Department of Physics Education, Faculty of Teacher Training and Education, Universitas Sebelas Maret, Surakarta 57126, Central Java, Indonesia
3. Centre of Excellence for Electrical Energy Storage Technology, Universitas Sebelas Maret, Surakarta 57146, Central Java, Indonesia

* corresponding author : elhanif@staff.uns.ac.id

Received : 05-14-2022; Revised : 06-10-2022; Accepted : 06-12-2022; Published : 06-27-2022.

ABSTRACT: The development of Li-ion batteries leads to high-density Li-ion battery technology as a storage system. to realize a Li-ion battery with a high energy density is to modify its anode, called a thin-film anode. The anode used is coated with a material thickness of 10 μm, increasing the cathode material that can be accommodated in one cell. This study aimed to analyze the Cu-powder and LTO materials used in Thin-film Li-ion batteries as a substitute for graphite because they offer higher capacity, chemical stability, fast charging technology (LTO), cheap, and environmentally friendly (Cu-powder). Based on XRD and FTIR tests, the material has a good crystal structure, and not many impurities are still contained in it. The SEM results showed that both particles showed uniformity in the shape of a single particle and were strengthened by the SEM-EDX test to review the quantity of each element present in the two materials. The electrochemical test results showed that Cu-powder material was better, with a specific capacity of 144.82 mAh $g^{-1,}$ higher than LTO (81.04 mAh g^{-1}).

Keywords: high-density energy, Cu-powder, LTO, Thin-film anode, Li-ion battery

1. Introduction

Li-ion is becoming a significant player in rechargeable energy storage technology. Li-ion batteries are chosen as the primary energy source for portable devices such as mobile phones, laptops, and power tools. They are now being applied to electric vehicles such as e-bikes, motorcycles, and electric cars [1]. Rapid technological developments encourage improvements in the Li-ion battery energy storage system. High-density energy Li-ion batteries are a new challenge in developing Li-ion batteries because, in the same cell, they must produce a greater energy density [2]. Li-ion batteries consist of four parts: cathode, anode, separator, and electrolyte. One of the things that can be done to realize a high-density Li-ion battery is to modify the electrodes.

The modified electrode is the anode. The anode is the electrode's negative side, a reducing agent [3]. The anode has a vital role in the performance of Li-ion batteries because it affects the cycle performance,

battery charge rate, and energy density, so the selection of anode material is very important [4]. The dendritic phenomenon is another reason for the importance of choosing anode material. Dendrite is the accumulation of Li ions that cannot be recalculated back to the cathode side, called dead-Li [5].

Graphite is an anode material that has been used commercially in Li-ion batteries. The electrochemical activity of the carbon material comes from the intercalation process of Li ions between the graphene planes, which provides good mechanical stability, electrical conductivity, and Li transport. Carbon materials balance cost factors with good electrochemical activity [6]. However, the low specific capacity of carbon materials is the reason for the emergence of alternative anode materials for lithium-ion batteries [7]. Graphite materials also have limitations in filling rates. At high charging rates, the graphite material has the potential to short-circuit, which affects battery safety. This is due to the emergence of a lithiation effect in the form of the appearance of dendrites on the anode layer due to the one-dimensional intercalation space of the graphite material [8]. The Li^+ ion intercalation voltage is so low (<0.25 V vs. Li/Li^+) that Li metal can quickly form a layer on the graphite surface when charging Li-ion batteries, especially at high currents and cold temperatures. The Li-coated graphite reacts with the electrolyte solvent, which can degrade battery performance and form dendrites, posing a potential safety hazard. Other disadvantages of carbon anode materials are 10 - 20% irreversible capacity in the first cycle due to SEI formation, low density affecting the battery's volumetric energy density, and unsuitability for fast charging due to possible Li coating [9]. Therefore, the development of anode materials leads to graphite replacement materials using several material sources such as carbon nanomaterials, silicon, and transition group metals (Fe, Co, Ni, Sn, Cu, etc.) [10].

Cu transition metal group as an anode can improve the performance of Li-ion batteries. The use of Cu material can maximize the capacity and cycle stability of Li-ion batteries [10]. Another advantage offered is that it provides excellent performance stability at a low price, is easy to obtain, has a high theoretical capacity, and is environmentally friendly [11], [12]. Another potential material for graphite substitute is Lithium Titanate ($Li_4Ti_5O_{12}$). Lithium Titanate (LTO) has good structural stability without changes in structure or volume during the lithiation/de-lithiation process (charging and discharging process) [13]. Therefore, the LTO anode material is classified as a non-strain material and has a capacity of 175 mAh g^{-1} [14]. The high crystallinity of LTO is the advantage of this material, especially for its electrochemical performance. Synthesis of LTO anode material can use several methods. The methods used are sol-gel, molten salt, spray pyrolysis, hydrothermal, and solid-state [15]. The sol-gel method was used to synthesize LTO at low temperatures. To achieve high LTO crystallinity, the molten-salt method can be used. However, the final product synthesized using the molten-salt method requires a washing process to remove the salt content. As a result, much wastewater containing lithium salts will be wasted in the environment [16]. The hydrothermal method used for the synthesis of LTO can be an option. However, the process in this method requires high temperatures and pressures to reach a critical point so it will require a large amount of energy [17]. The solid-state method is a choice that is considered. This method is the most straightforward and efficient method of mixing raw materials in the solid phase [15].

This research will discuss the comparative study of novelty thin films for Li-ion batteries. The use of thin-film Cu (Cu-powder) and LTO anode materials attempts to increase the energy density in one battery cell. By decreasing the thickness of the anode, the amount of cathode material that can be inserted into the battery becomes more so that it can increase the energy density in one battery cell. The conclusion that will be drawn in this research is which material is better than other materials when applied as thin-film anodes for high-energy-density Li-ion batteries.

2. Methodology

2.2. Material synthesis and preparation

The primary materials used in this research are Cu powder and LTO. Cu powder was obtained from Polimikro Berdikari Nusantara, Ltd (Polimikro Berdikari Nusantara, Ltd., Indonesia). The LTO material was obtained by synthesis using the solid-state method. The materials used are TiO_2, Methanol from Agung Jaya, Ltd. (Agung Jaya, Ltd., Indonesia), and $LiOH.H_2O$ from Leverton (Leverton, UK). The cathode material used is NMC622 from Gelon (Gelon, China). The schematic of the LTO material synthesis is illustrated in Fig. 1. TiO_2 as a source of Ti and LiOH as a source of Li were mixed in a solid-state with a mole ratio of Li: Ti = 4:5, and the mixing process was assisted with methanol as a dispersant. The solid-state mixing process uses a stirrer with a rotational speed of 1000 rpm for 2 hours. This stirring process is carried out until the reaction is perfectly marked by a change in temperature to cold in the mixed material. The mixed material is dried to evaporate methanol in an oven to dry to form a precursor. The precursors were heated and sintered under O_2 conditions at 800° C for 12 hours. After the sintering process is complete, the LTO product is cooled, and the final step is size reduction to 200 mesh. The material was tested for XRD, FTIR, SEM, and electrochemical performance tests.

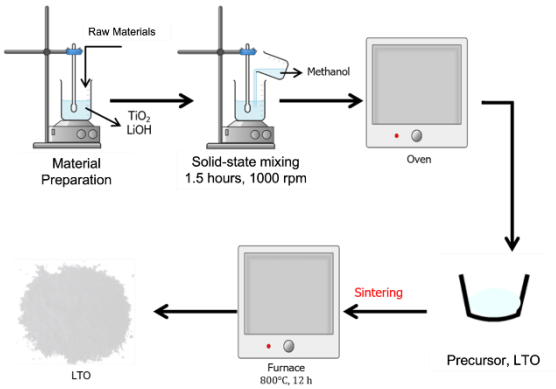

Figure 1. Synthesis scheme for LTO material

2.3. Coating and battery manufacturing

Cu-powder and LTO materials were applied as Thin-film anodes in high energy density Li-ion batteries. These two materials are coated on the surface of Cu-foil with a thickness of 10 μm as Li-host. XRD and FTIR test results show that both materials have good crystallinity and few impurities. Morphological SEM and EDX tests showed uniformity of particle shape with an average size of 8.78 μm Cu-powder, 1.69 μm, and agglomeration appeared to occur in the LTO material. At a current of 0.1 C, the electrochemical performance test showed that Cu-powder material was better than LTO with the first specific capacity of 144.82 mAh g^{-1} compared to LTO 81.04 mAh g^{-1} the cycle stability test of Cu-powder material was more stable than LTO material.

3.3.Testing

Cu-powder and LTO materials were applied as Thin-film anodes in high energy density Li-ion batteries. These two materials are coated on the surface of Cu-foil with a thickness of 10 μm as Li-host. XRD and FTIR test results show that both materials have good crystallinity and few

impurities. Morphological SEM and EDX tests showed uniformity of particle shape with an average size of 8.78 µm Cu-powder, 1.69 µm, and agglomeration appeared to occur in the LTO material. At a current of 0.1 C, the electrochemical performance test showed that Cu-powder material was better than LTO with the first specific capacity of 144.82 mAh g^{-1} compared to LTO 81.04 mAh g^{-1} the cycle stability test of Cu-powder material was more stable than LTO material.

3.3. Result and Discussion

3.1. Materials Characterization

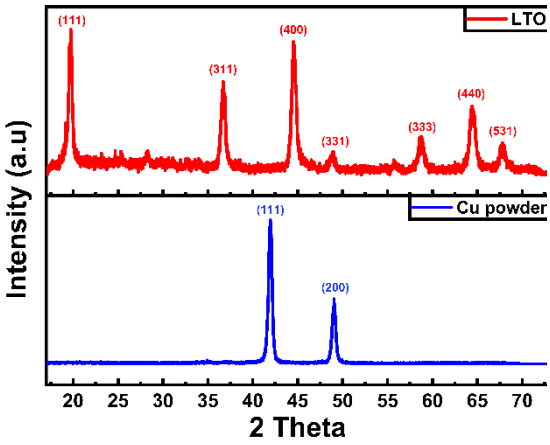

Figure 2. XRD pattern for Cu powder and LTO materials

X-Ray Diffraction (XRD) analysis is one of the solid materials or materials research characteristics. XRD test aims to determine the phase of a crystal and the impurity of the material produced. Fig. 2 is the XRD pattern for the Cu-powder sample and LTO product, including the miller index. XRD pattern of Cu-powder material in the first row shows two main peaks of Cu, namely peaks (111) and (200), at two theta angles of 41.95° and 49.04° [18], [19]. This shows that the material is indeed Cu-powder, and there are no impurities in it. The second line has the XRD pattern of LTO materials synthesized by the solid-state method. The results show that all significant LTO material peaks appear compared to ICDD-LTO data. The LTO peaks that appear are peaks (111), (311), (400), (331), (333), (440), and (531) with two theta angles of 19.70°, 36.71°, 44.58°, 48.83°, 58.75°, 64.45°, and 67.81° [20], [21]. There is a little noise on the curve, but it does not indicate significant impurities. The two XRD patterns of each material show sharp peaks so that the material has a high level of crystallinity [20]–[22].

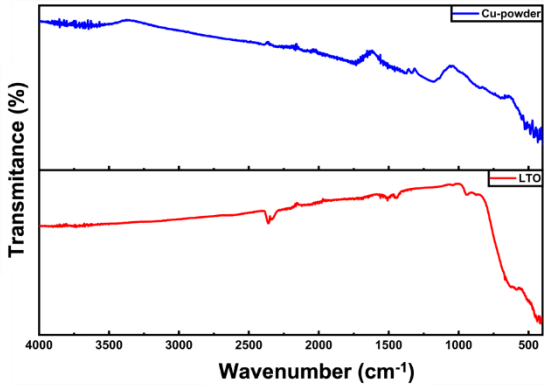

Figure 3. FTIR spectrum for Cu powder and LTO materials

FTIR spectrum analysis analyzes the organic functional groups present on the particle surface. This functional group makes it possible to determine the carbon bonds still left behind as impurities and determine the bonds that occur in the main product [23]. Fig. 3 displays the FTIR spectrum for Cu-powder and LTO materials. The FTIR spectrum of Cu-powder material in the first row shows four peaks. The first peak at wavenumber 1732.94 cm^{-1} indicates the presence of a C=C alkene group. The second peak at wavenumber 1185 cm^{-1} indicates the presence of a C-O group and a C-H group seen at wavenumber 738.82 cm^{-1}. The fourth peak at wavenumber 486.36 cm^{-1} indicates the presence of the Cu-O functional group [24]–[26]. There is a Cu-O bond group, and carbon functional groups dominate other functional groups. The second FTIR spectrum is LTO material, which shows five peaks. The peaks at wavenumbers 486.36

and 586.21 cm^{-1} indicate the presence of a symmetrical and asymmetrical spectrum of the stretching octahedral group so that it can be ascertained that there is a spinel LTO peak [21]. The FTIR spectrum at wavenumber 937.07 cm^{-1} represents the presence of C-O groups [27] and wavenumber 1473.36 cm^{-1} represents the spectrum of carboxyl groups $-CH_2$, respectively [28].

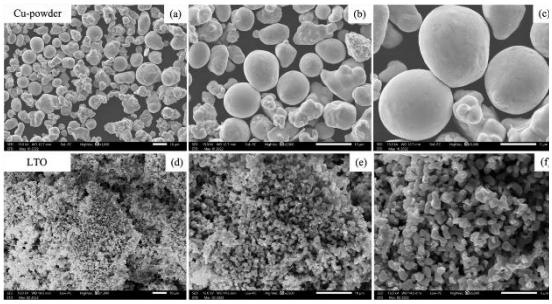

Figure 4. SEM-surface morphology for Cu powder materials with (a) x1000 magnification, (b) x2500 magnification, (c) x5000 magnification and SEM-surface morphology for LTO materials with (a) x1000 magnification, (b) x2500 magnification, (c) x5000 magnification

Scanning Electron Microscopy (SEM) morphology aims to determine the surface morphology of the appearance of the particles analyzed at x1000, x2500, and x5000 magnifications. The first three line drawings in Fig. 4 (a), (b), and (c) are the results of the surface morphology analysis of the Cu-powder material. At x1000 magnification, the particles have a uniform spherical shape. No agglomeration occurs between Cu-powder particles at high magnification (x2500 and x5000). Particle size analysis based on surface morphology, Cu-powder has an average particle size of 8.78 μm. The three second-row images in Fig. 4 (d), (e), and (f) are SEM results of the surface morphology of the LTO material. There is uniformity of particle shape but visible agglomeration, which is visible at x5000 magnification. The average size of a single LTO particle is 1.69 μm. SEM-EDX (Energy Dispersive X-ray) analysis was also carried out to determine the elemental content and impurities. This test will determine the purity and mass percentage of the elements present in the tested material. Fig. 5 (a) shows the energy spectrum of the Cu-powder material, and Fig. 5 (b) shows the energy spectrum of the CuO material. Fig. 5 is reinforced by the description in Table 1, which contains the percentage of mass contained in both samples. Fig. 5 (a) high Cu-La peaks are seen. This indicates the high intensity of energy absorbed due to the presence of Cu, which shows a high Cu content compared to the C and O content at the peaks of C-Ka and O-Ka.

Table 1. The mass percentage of Cu-powder and LTO elements from SEM-EDX analysis

Elements	Mass Percentage (%)	
	Cu Powder	LTO
Cu	95.01	0
O	1.08	67.11
C	3.91	0
Ti	0	32.89

The data from Table 1 reinforce this; the percentage of the mass of the element Cu is 95.01%m. Fig. 5 (b) shows two main peaks, Ti-Ka and O-Ka, with an insignificant difference in peak heights. Mass percentage of Ti : O = 32.89 : 67.11. The number of elements O is more than the element Ti. this is in line with the chemical formula LTO ($Li_4Ti_5O_{12}$), which shows the composition and quantity percentage by mass of element O is more than element Ti.

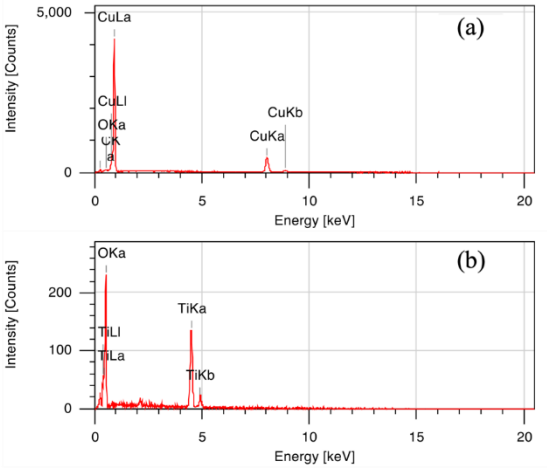

Figure 5. Energy-dispersive X-ray for Cu powder and LTO materials

3.2. Electrochemical Performance Test

The electrochemical performance test was carried out in a fully 18650 cylindrical cell. The cathode used was NMC622, with a theoretical specific capacity of 200 mAh g^{-1}. The electrochemical tests reviewed the performance of the first three cycles of specific charge/discharge capacity and the stability of the cycle up to the 50th cycle. Fig. 6 (a) shows the charge/discharge curve of the first three battery cycles using Cu-powder as anode material. Fig. 6 (b) shows the results for a battery with LTO anode material. It can be seen that the first three cycles of these two batteries differ quite a lot. The first capacity is 144.83 mAh g^{-1} which increases in the second cycle to 153.33 mAh g^{-1}. This value is greater than the battery using LTO material with the first specific capacity of 96.77 mAg g^{-1} and a drop of 81 mAh g^{-1} in the third cycle. The superiority of the Cu material is reinforced by cycle stability data that is tested up to 50 cycles. Fig. 6 (c) shows the results of the second cycle stability test of anode material. The initial capacity of Cu powder material is strengthened with good stability in the first five cycles compared to LTO material. The LTO material drops, and the capacity runs out in the 19th cycle. At the same time, the battery with Cu powder drops in the 41st cycle. LTO materials are generally stable at a voltage of 2.3 V. However, the results of this study show a tendency to form the same curve and are stable at a voltage of 3.8 V. Therefore, the battery performance shown by both the Cu-powder and LTO materials which are thinly coated with a thickness of 10 micrometers is close to anode-free Li-ion battery performance.

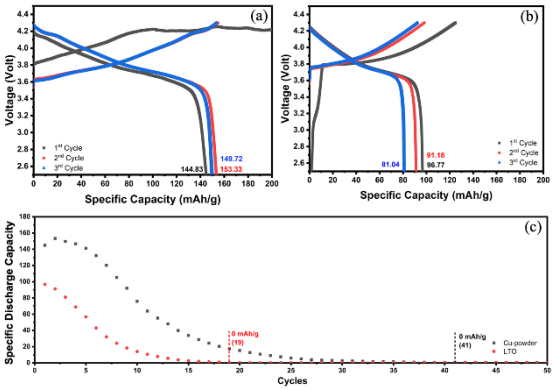

Figure 6. (a) The first three cycles of the charge/discharge specific capacity curve of the battery with Cu powder, (b) The first three cycles of the charge/discharge specific capacity curve of the battery with LTO, and (c) The first fifty cycles of stability for Cu powder and LTO anode-poor

4. Conclusions

Cu-powder and LTO materials were applied as Thin-film anodes in high energy density Li-ion batteries. These two materials are coated on the surface of Cu-foil with a thickness of 10 µm as Li-host. XRD and FTIR test results show that both materials have good crystallinity and few impurities. Morphological SEM and EDX tests showed uniformity of particle shape with an average size of 8.78 µm Cu-powder, 1.69 µm, and agglomeration appeared to occur in the LTO material. At a current of 0.1 C, the electrochemical performance test showed that Cu-powder material was better than LTO with the first specific capacity of 144.82 mAh g-1 compared to LTO 81.04 mAh g-1 the cycle stability test of Cu-powder material was more stable than LTO material.

5. Acknowledgment:

We acknowledge Indonesia Endowment Fund for Education (LPDP / Lembaga Pengelola Dana Pendidikan) for the support through Pendanaan Riset Inovatif Produk (Rispro) Invitasi grant no.PRJ-6/LPDP/2020.

References

[1] S. Chu, Y. Cui, and N. Liu, "The path towards sustainable energy," *Nature Materials*, vol. 16, no. 1, pp. 16–22, 2016, DOI: 10.1038/nmat4834.

[2] Y. Qiao, H. Yang, Z. Chang, H. Deng, X. Li, and H. Zhou, "A high-energy-density and long-life initial-anode-free lithium battery enabled by a Li2O sacrificial agent," *Nature Energy*, vol. 6, no. 6, pp. 653–662, 2021, DOI: 10.1038/s41560-021-00839-0.

[3] J. B. Goodenough and K. S. Park, "The Li-ion rechargeable battery: A perspective," *J Am Chem Soc*, vol. 135, no. 4, pp. 1167–1176, 2013, DOI: 10.1021/ja3091438.

[4] D. Deng, "Li-ion batteries: Basics, progress, and challenges," *Energy Science and Engineering*, vol. 3, no. 5. John Wiley and Sons Ltd, pp. 385–418, Sep. 01, 2015. DOI: 10.1002/ese3.95.

[5] Q. Li *et al.*, "Homogeneous Interface Conductivity for Lithium Dendrite-Free Anode," *ACS Energy Letters*, vol. 3, no. 9, pp. 2259–2266, 2018, doi: 10.1021/acsenergylett.8b01244.

[6] N. Nitta, F. Wu, J. T. Lee, and G. Yushin, "Li-ion battery materials : present and future," *Biochemical Pharmacology*, vol. 18, no. 5, pp. 252–264, 2015, DOI: 10.1016/j.mattod.2014.10.040.

[7] R. Li, W. Yue, and X. Chen, "Fabrication of porous carbon-coated ZnO nanoparticles on electrochemical exfoliated graphene as an anode material for lithium-ion batteries," *Journal of Alloys and Compounds*, vol. 784, pp. 800–806, May 2019, DOI: 10.1016/j.jallcom.2019.01.117.

[8] J. Ginting, E. Yulianti, and Sudaryanto, "SINTESIS Li2TiO3 SEBAGAI BAHAN ANODA BATERAI Li-ION DENGAN METODE REAKSI PADATAN," *Jurnal Sains Materi Indonesia*, vol. 15, 2014.

[9] Z. Zhang, Y. Wang, J. Hu, Q. Wu, and Q. Zhang, "Influence of mixing method and hydraulic retention time on hydrogen production through photo-fermentation with mixed strains," *International Journal of Hydrogen Energy*, vol. 40, no. 20, pp. 6521–6529, 2015, DOI: 10.1016/j.ijhydene.2015.03.118.

[10] W. Xu *et al.*, "Lithium metal anodes for rechargeable batteries," *Energy and Environmental Science*, vol. 7, no. 2, pp. 513–537, 2014, DOI: 10.1039/c3ee40795k.

[11] R. Dang, X. Jia, X. Liu, H. Ma, H. Gao, and G. Wang, "Controlled synthesis of hierarchical Cu nanosheets @ CuO nanorods as high-performance anode material for lithium-ion batteries," *Nano Energy*, vol. 33, pp. 427–435, 2017, DOI: 10.1016/j.nanoen.2017.01.024.

[12] S. H. Lee, Y. Noh, Y. R. Jo, Y. Kim, B. J. Kim, and W. B. Kim, "Carbon-Encapsulated SnO2 Core–Shell Nanowires Directly Grown on Reduced Graphene Oxide Sheets for High-Performance Li-Ion Battery Electrodes," *Energy Technology*, vol. 6, no. 7, pp. 1255–1260, 2018, DOI: 10.1002/ente.201700804.

[13] L. Lu, Y. Hu, and K. Dai, "The advance of fiber-shaped lithium ion batteries," *Materials Today Chemistry*, vol. 5, pp. 24–33, 2017, DOI: 10.1016/j.mtchem.2017.05.003.

[14] M. Odziomek *et al.*, "Hierarchically structured lithium titanate for ultrafast

charging in long-life high capacity batteries," *Nature Communications*, vol. 8, no. May, pp. 1–7, 2017, DOI: 10.1038/ncomms15636.

[15] A. Purwanto *et al.*, "High performance of salt-modified–to anode in lifepo4 battery," *Applied Sciences (Switzerland)*, vol. 10, no. 20, pp. 1–15, 2020, DOI: 10.3390/app10207135.

[16] S. Y. Yin *et al.*, "Molten salt synthesis of sodium lithium titanium oxide anode material for lithium ion batteries," *Journal of Alloys and Compounds*, vol. 642, pp. 1–6, 2015, DOI: 10.1016/j.jallcom.2015.04.113.

[17] Y. Sha, B. Zhao, R. Ran, R. Cai, and Z. Shao, "Synthesis of well-crystallized Li4Ti5O12 nanoplates for lithium-ion batteries with outstanding rate capability and cycling stability," *Journal of Materials Chemistry A*, vol. 1, no. 42, pp. 13233–13243, 2013, DOI: 10.1039/c3ta12620j.

[18] Y. Chu, M. Chen, S. Chen, B. Wang, K. Fu, and H. Chen, "Micro-copper powders recovered from waste printed circuit boards by electrolysis," *Hydrometallurgy*, vol. 156, pp. 152–157, Jun. 2015, DOI: 10.1016/j.hydromet.2015.06.006.

[19] J. Temuujin *et al.*, "Preparation of copper and silicon/copper powders by a gas evaporation-condensation method," *Bulletin of Materials Science*, vol. 32, no. 5, pp. 543–547, Nov. 2009, DOI: 10.1007/s12034-009-0081-1.

[20] P. Hosseini, "Comparative study between Li4Ti5O12 and Pr doped Li4Ti5O12 in Li-Sulfur battery with Li2S cathodic electrode," 2017. [Online]. Available: https://www.researchgate.net/publication/321801918

[21] B. Vikram Babu *et al.*, "Structural and electrical properties of Li4Ti5O12 anode material for lithium-ion batteries," *Results in Physics*, vol. 9, pp. 284–289, Jun. 2018, DOI: 10.1016/j.rinp.2018.02.050.

[22] S. Priyono, B. M. Lubis, S. Humaidi, and B. Prihandoko, "Heating Effect on Manufacturing Li4Ti5O12 Electrode Sheet with PTFE Binder on Battery Cell Performance," in *IOP Conference Series: Materials Science and Engineering*, Jun. 2018, vol. 367, no. 1. doi: 10.1088/1757-899X/367/1/012007.

[23] R. Betancourt-Galindo *et al.*, "Synthesis of Copper Nanoparticles by Thermal Decomposition and Their Antimicrobial Properties," *Article in Journal of Nanomaterials*, vol. 2013, 2013, DOI: 10.1155/2013/980545.

[24] Z. Janković, M. M. Pavlović, M. R. P. Pavlović, N. D. Nikolić, V. Zečević, and M. G. Pavlović, "Electrical conductivity of poly (L lactic acid) and poly (3-hydroxybutyrate) composites filled with galvanostatically produced copper powder," *Hemijska Industrija*, vol. 72, no. 5, pp. 285–292, 2018, DOI: 10.2298/HEMIND180530020J.

[25] N. B. Tanvir, O. Yurchenko, C. Wilbertz, and G. Urban, "Investigation of CO2 reaction with copper oxide nanoparticles for room temperature gas sensing," *Journal of Materials Chemistry A*, vol. 4, no. 14, pp. 5294–5302, 2016, DOI: 10.1039/c5ta09089j.

[26] M. Moyo, G. Nyamhere, E. Sebata, and U. Guyo, "Kinetic and equilibrium modelling of lead sorption from aqueous solution by activated carbon from goat dung," *Desalination and Water Treatment*, vol. 57, no. 2, pp. 765–775, Jan. 2016, DOI: 10.1080/19443994.2014.968217.

[27] C. K. Lan, C. C. Chang, C. Y. Wu, B. H. Chen, and J. G. Duh, "Improvement of the Ar/N2 binary plasma-treated carbon passivation layer deposited on Li4Ti5O12 electrodes for stable high-rate lithium ion batteries," *RSC*

Advances, vol. 5, no. 112, pp. 92554–92563, 2015, DOI: 10.1039/c5ra17522d.

[28] J. Gao, B. Gong, Q. Zhang, G. Wang, Y. Dai, and W. Fan, “Study of the surface reaction mechanism of Li4Ti5O12 anode for lithium-ion cells,” *Ionics (Kiel)*, vol. 21, no. 9, pp. 2409–2416, Sep. 2015, DOI: 10.1007/s11581-015-1435-x.